proach zero at 90°), we obtain a Group 2 cesium ion flux of about 10^{12} ions/cm²-sec.

Hall[4] presents the following equation for target erosion rate, which he states to hold after an initial period during which the target is becoming saturated with propellant atoms

$$dx/dt = \Gamma S/n \quad (12)$$

where dx/dt is the rate of change of target thickness with respect to time (cm/sec); B is the bombarding ion flux density (ions/cm²-sec); S is the sputtering yield (target atoms/ion); and n is the target number density (atoms/cm³). Daley[7] presents data that show that the sputtering yield is about one atom per incident ion for an energy of 600 ev. The primary flux at the cesium thruster exhaust is 1.8×10^{16} ions/cm²-sec. The corresponding erosion rate is 3×10^{-7} cm/sec or about 1 cm/1000 hr. As an approximation, erosion rates at other positions may be determined as a direct ratio with the flux.

If we apply the approximation to Group 2 ions, it will be conservative since the average ion energy is lower than the Group 1 ions. This means that, on the average, fewer atoms are sputtered per ion impacting on the surface. The Group 2 ion flux of 10^{12} therefore erodes about 4×10^{-5} cm/1000 hr. This is a very small amount and should not be a problem for a solid surface. However, it may be significant for a surface such as aluminized Mylar. A more detailed investigation would be indicated if such a surface were located close to the thruster.

Conclusions

Conditions exist in some spacecraft where it is incorrect to neglect the charge exchange ions in evaluating the effect of ion thruster exhaust. Low temperature surfaces that are recessed into the spacecraft may be particulary sensitive because of directional effects. A very gross analysis also indicates that sputtering due to Group 2 ions might be a problem for thin films. Further work is indicated in this area.

The problems could be eliminated in the analyzed spacecraft by two changes: 1) recess the thruster into the spacecraft so that the exhaust opening cannot be seen from the spacecraft, and 2) charge the thruster neutralizer to about 50 or 100 v to prevent Group 4 ions from reaching the spacecraft. The former eliminates direct impingement of neutral atoms and Group 2 ions upon the spacecraft. The latter provides sufficient potential difference that the low energy Group 4 ions cannot penetrate to the spacecraft.¶

References

[1] Reynolds, T. and Richley, E. A., "Propellant Condensation on Surfaces near an Electric Rocket Exhaust," *Journal of Spacecraft and Rockets*, Vol. 6, No. 10, Oct. 1969, pp. 1155–1161.

[2] Staggs, J. F., Gula, W. P., and Kerslake, W. R., "Distribution of Neutral Atoms and Charge-Exchange Ions Downstream of an Ion Thruster," *Journal of Spacecraft and Rockets*, Vol. 5, No. 2, Feb. 1968, pp. 159–164.

[3] "A Study of Cesium Exhaust from an Ion Engine and Its Effect upon Several Spacecraft Components," HIT-399, June 1969, Hittman Associates, Inc., Columbia, Md.

[4] Hall, D. F., Newnam, B. E., and Womack, J. R., "Electrostatic Rocket Exhaust Effects on Solar-Electric Spacecraft Subsystems," *Journal of Spacecraft and Rockets*, Vol. 7, No. 3, March 1970, pp. 305–312.

[5] Sohl, G., Reid, G. C., and Speiser, R. C., "Cesium Electron Bombardment Ion Engine," *Journal of Spacecraft and Rockets*, Vol. 3, No. 7, July 1966, pp. 1093–1098.

[6] Sellen, J. M., Jr., Kemp, R. F., and Hieler, R. H., "Observations of Neutralized Ion Thrust Beams in the 25-Meter NASA Testing Chamber," CR-53634, 1964, TRW, NASA.

[7] Daley, H. L. and Perel, J., "Cesium Ion Sputtering of Aluminum, Copper, and Titanium, AIAA Paper 66-203, San Diego, Calif., 1966.

¶ Staggs[2] believes the energy of these charge exchange ions is less than about 50 v. Sellen[6] gives a 7 or 8 v potential across a beam. Beam potentials of less than 10 v relative to the ion source are reported.

Total Emittance Measurements of Thin Metallic Films at Cryogenic Temperatures

G. R. CUNNINGTON* AND G. A. BELL†
Lockheed Palo Alto Laboratory, Palo Alto, Calif.

AND

B. F. ARMALY‡ AND C. L. TIEN§
University of California, Berkeley, Calif.

Nomenclature

A	=	sample frontal area = absorber
a_b	=	blackbody absorptance ≈ 0.98
a_s	=	sample absorptance for blackbody radiation at T_b and sample at T_s; a'_s, same, but sample at T_c
F	=	sample to blackbody view factor = blackbody to sample view factor
T_b	=	blackbody absorber temperature
T_c	=	sample temperature during calibration ≈ 20 or 77°K
T_s	=	sample temperature
Q_c	=	calibration power input
Q_l	=	heat flux to blackbody thermal link
Y_c, Y_s	=	blackbody radiation exchanges with wall during calibration and during sample run
ϵ_b	=	blackbody emittance at $T_b \approx 0.98$
ϵ_s, ϵ_s'	=	sample emittances at T_s and at T_c, respectively
σ	=	Stefan-Boltzmann's constant

Introduction

THE most efficient multilayer insulation reflective shield concept uses vacuum-deposited gold or aluminum (~500 Å) on a very thin plastic sheet (0.15 to 0.25 mils thick) such as Mylar or Kapton which greatly reduces system weight[1] and thermal anisotropy[2] of the insulation over one using metal foils. The first theoretical work on the radiation properties of thin metallic films[3] was based upon the Drude single (or free) electron (DSE) theory of optical constants. However, it later became apparent that the anomalous skin effect (ASE) theory[4] should be used rather than the DSE theory for the cryogenic temperature range. The recent work of Domoto et al.[5] showed that the predicted values of total hemispherical emittance ϵ based upon the ASE theory could be an order of magnitude greater than those predicted by the DSE theory. It has been shown[6,7] for the condition when the film thickness becomes smaller than the electron mean free path that the electrical and thermal properties of the film will differ from those of the bulk metal. To incorporate the size effect (i.e., influence of film thickness) into the skin effect, Dingle[8] established the theoretical framework for evaluating the radiative properties of thin metallic films on the basis of the ASE theory. An extensive analysis of size and skin effect at cryogenic temperatures has recently been done by Armaly and Tien.[9]

This Note reports measurements of ϵ for vacuum-deposited, high-purity gold films on plastic and metal substrates over the temperature range of 60–300°K. Effect of film thickness on ϵ

Presented as Paper 70-63 at the AIAA 8th Aerospace Sciences Meeting, New York, January 19–21, 1970; submitted March 5, 1970; revision received September 4, 1970. The authors are grateful to M. McCargo and S. A. Greenberg, who provided the proton transmission measurements, and to D. A. Vance for preparation of gold on copper specimens. Work at the University of California conducted under NASA Grant NGR-05-003-295, Ames Research Center, Moffet Field, Calif.

* Staff Scientist. Member AIAA.

† Senior Scientist.

‡ Presently at Department of Mechanical and Aerospace Engineering, University of Missouri, Rolla, Mo. Member AIAA.

§ Professor of Mechanical Engineering. Associate Fellow AIAA.

is demonstrated, and data are compared with theoretical results.

Experimental Apparatus and Procedure

The calorimetric emittance apparatus consists of a $2\frac{1}{2}$-in. diam by $\frac{3}{16}$-in. thick aluminum, brass, or copper sample substrate mounted to a liquid-nitrogen- or liquid-hydrogen-cooled vacuum chamber (Fig. 1). Sample temperature is controlled from cryogen temperature to 300°K using a spiral wound heater imbedded in a $2\frac{1}{4}$-in. diam copper heating block. Temperature is read out by a Rosemount Engineering Company 104 AH1 platinum resistance thermometer.

Radiated sample energy is collected using a blackbody absorber mounted to the cryogenically cooled supporting structure within 30 mils of the sample front face. This absorber consists of a series of thin wall metal tubes ($\frac{3}{16}$-in. o.d. by 10-mil wall by 1-in. long) fitted to the interior of an aluminum shell. The inside of the shell and tubes are coated with Cat-a-Lac flat black epoxy paint. The geometry of the blackbody coupled with the high absorptance of the paint leads to a calculated theoretical absorptance of 0.97. The blackbody thermal link is selected so that absorbed sample energy raises blackbody temperature between 5 and 10°K above that of the bath once thermal equilibrium is reached. For the present experiments, two thermal links were needed: three 20-mil diam stainless steel wires were used for sample temperatures between 60 and 160°K, while a $\frac{1}{4}$-in. o.d. by 20-mil wall stainless tube was used for sample temperatures between 160 and 300°K. Blackbody temperature is monitored using a platinum or germanium resistance thermometer.

The blackbody absorber is calibrated by allowing the sample to cool to cryogenic bath temperature, and supplying heat energy to the absorber through a carbon resistance heater. Once blackbody thermal equilibrium is attained, the power dissipated in the carbon resistor is measured and the temperature (thermometer resistance) is recorded. The process is then repeated for different power levels, and a curve of blackbody temperature vs power input to the blackbody can be generated. This technique produces a very reproducible curve since the blackbody thermal link and all the leads to the resistances mounted on its back face are thermally grounded to the cryogenic bath.

Preparation of specimens

The three gold on Mylar and one gold on Kapton specimens were taken from commercially prepared metallized materials; the Mylar specimens were metallized on both sides and the Kapton on only one side. For these the purity of the gold used for evaporation, the deposition rate, and the chamber pressure during evaporation are not known. The 400, 520, and 4000 Å gold on copper specimens were prepared at Lockheed from 99.999% purity gold. Deposition rate was 20–50 Å/sec and chamber pressure $\sim 10^{-6}$ torr. The substrate was highly polished brass over which 1000 Å of copper was deposited. The 2500 Å specimen¶ was prepared using gold of 99.999% purity; chamber pressure was 10^{-5} torr; deposition rate was 180 Å/sec. No determinations were made of the composition of the "as deposited" films.

Metal film thicknesses were measured for the three-coated Mylar specimens and three of the gold-copper specimens using a technique which measures transmission of a proton beam through the gold film as a function of the incident proton energy. The film thickness is determined from accurately calibrated energy vs thickness relationships for a proton/gold system.[10] This method itself yields thicknesses that are accurate to ±50 Å; however, the actual emittance samples were not used to make the measurements. The measurements of the Mylar specimens were made using an adjacent piece of the same section of film from which the emittance samples were taken. Since thicknesses across the section have been observed to vary by 200 Å or more, one should be careful in drawing conclusions concerning film thickness vs emittance on films whose thickness difference is less than 200 Å. For the 400, 520, and 4000 Å gold on copper specimens, film thickness was inferred from measurements made on quartz plates placed on two sides of the substrate during the deposition process. As these were immediately adjacent to the emittance specimen, it is believed these thickness values are representative of the actual emittance specimen. Thicknesses for the Kapton and the 2500 Å gold on copper specimens were provided by the supplier.

¶ Sample supplied by Alan P. Bradford, Department of the Army, Night Vision Lab., Fort Belvoir, Va.

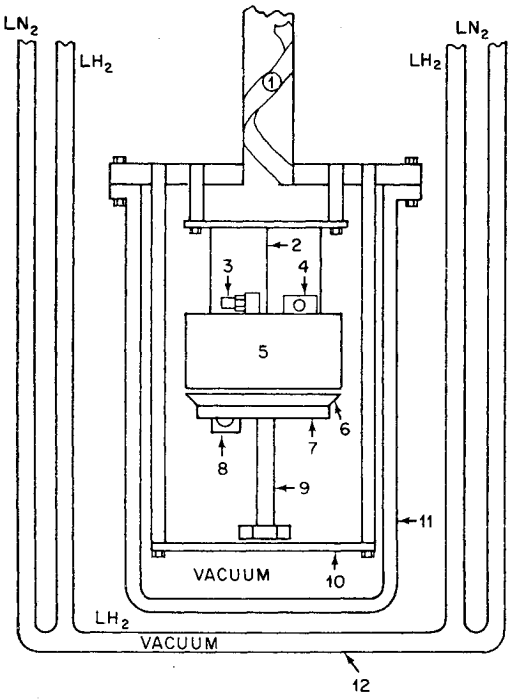

Fig. 1. Experimental apparatus. 1) Copper radiation strap; 2) blackbody thermal link (three 20-mil stainless wires); 3) germanium resistance thermometer; 4) blackbody heater; 5) blackbody absorber; 6) sample substrate; 7) sample heater; 8) platinum resistance thermometer; 9) sample thermal link; 10) copper supporting structure; 11) vacuum-tight experimental chamber; 12) double wall dewar.

With a radiating sample present, the heat flux reaching the blackbody thermal link is equal to the radiated sample energy, which is absorbed by the blackbody, minus the radiated blackbody energy, which is either absorbed by the sample or the chamber walls. Therefore:

$$Q_l = A\sigma T_s^4 F\{\epsilon_s a_b/[1 - F^2(1 - \epsilon_s)(1 - a_b)]\} - A\sigma T_b^4 F/\{\epsilon_b a_s/[1 - F^2(1 - \epsilon_b)(1 - a_s)]\} - Y_s \quad (1)$$

and during calibration the heat flux reaching the link is:

$$Q_l = Q_c - Q_r - Y_c \quad (2)$$

where:

$$Q_r = A\sigma T_b^4 F\{\epsilon_b a_s'/[1 - F^2(1 - \epsilon_b)(1 - a_s')]\} - A\sigma T_c^4 F\{\epsilon_s' a_b/[1 - F^2(1 - \epsilon_s)(1 - a_b)]\} \quad (3)$$

Although the sample absorptance for blackbody radiation at 20° or 77°K and the sample emittance at these temperatures are not known, the magnitude of Eq. (3) is negligible since $T_b \ll T_s$. Similarly, the second term on the right-hand side of Eq. (1) may be neglected. This introduces an error estimated at less than 1%. Also, $Y_c = Y_s$ as the blackbody

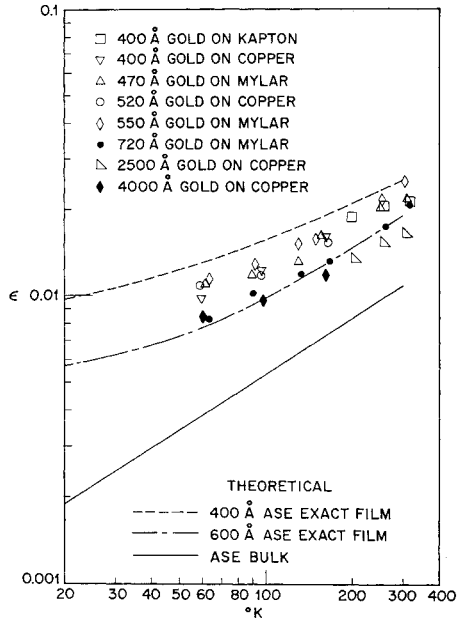

Fig. 2 Total hemispherical emittance vs temperature for gold films.

and wall temperatures are identical for calibration and sample runs.

Thus, Eq. (2) is reduced to

$$Q_c = A\sigma T_s^4 F\{\epsilon_s a_b/[1 - F^2(1 - \epsilon_s)(1 - a_b)]\} \qquad (4)$$

and ϵ_s can be calculated, since all the terms in Eq. (4) are known including a_b, which can be calculated using an iterative process and data obtained by substituting a blackbody radiator identical to the blackbody absorber for the sample. We found a_b to be 0.98 ± 0.01 from 80 to 260°K.

Error analysis

The probable errors ($\pm\Delta N$) for T_s, Q_c, and ϵ_s are shown in Table 1, and the $\Delta\epsilon_s$ values shown in Tables 1 and 2 were calculated as follows:

$$\Delta\epsilon_s = \epsilon_s(\mu_s/\epsilon_s)$$

$$= \epsilon_s[(4\Delta T_s/T_s)^2 + (\Delta Q_c/Q_c)^2 + (\Delta a_b/a_b)^2 + (\Delta F/F)^2]^{1/2}$$

As shown in Table 1, measurements at the lowest sample temperature are subject to the greatest uncertainty, principally because the ΔT between the blackbody absorber and the cryogen bath is approaching the same order of magnitude as the barometric pressure shifts at cryogenic liquid temperature. At the higher sample temperatures, the principal source of error is attributable to the ΔT's across the $2\frac{1}{2}$-in. diam sample.

A source of error which was not listed in Table 1 but which can be very significant is heat transfer to or from the blackbody absorber due to residual gas conduction. In the present experiments, great care was taken in designing and fabricating the experimental vacuum chamber so that pressures less than 10^{-8} torr could be realized. At the lowest sample temperature, it can be shown that heat transfer by residual gas conduction is of the same order of magnitude as heat transferred by radiation if the chamber pressure is of the order of 10^{-5} torr.

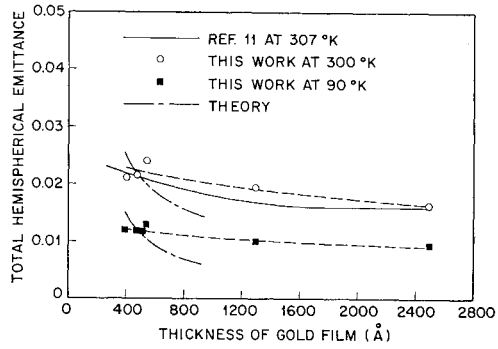

Fig. 3 Total hemispherical emittance of gold films vs film thickness for 300° and 90°K.

Results

Table 2 and Figs. 2 and 3 present the data. Measurements on the 400 Å film on Kapton and the 2500 Å film on copper specimens were performed at the University of California. All other data for this work were obtained at the Lockheed Palo Alto Research Laboratory. Figure 3 also includes a curve for room-temperature data from Ref. 11. While the experimental data seem to deviate appreciably from the theoretical results in Fig. 2, the general trend exhibited by the data does agree qualitatively with the prediction, and the consistency of data is impressive in view of the agreement between low-temperature data of two independent investigators (Lockheed and Berkeley) and the agreement among room temperature data of three investigations (Lockhead and Berkeley, and Ref. 11). The measured effect of film thickness is not as pronounced as that predicted by the theory, as is shown in Fig. 3. However, their study as well as this one clearly demonstrates a noticeable effect of film thickness on the total hemispherical emittance and, in addition, confirms the predicted trend of this effect.[9]

The substrate material (i.e., plastic or copper) does not appear to have a significant influence on emittance of the gold surface, even in the thin-film data shown in Fig. 2. This implies that gold films of thickness ~400 Å are nearly opaque for the primary wavelength range corresponding to the sample temperature. Therefore, the effect of film thickness on emittance is not due to the change in transparency but rather due to the restriction of electron free paths at the boundaries. The present thick-film data are limited to 2500 and 4000 Å films. The effect of still greater thickness should be negligible, since the film thickness will become much larger than the electron mean free path.[9] For instance, at room temperature the electron mean free path for gold is ~600 Å and the size effect becomes negligible for films of thicknesses larger than 1500 Å.

Caren's low-temperature emittance data for gold[12] are much higher than those reported here. The gold he used was chemically deposited, and no thickness was specified. The large discrepancy is probably due to the quality of the film used and possible differences in the experimental procedure.

The present data are about 50 or 100% higher (room temperature and 60°K cases, respectively) than the predicted values. This difference, which is much larger than the experimental errors of 3–8%, must be due to factors other than the thickness of the film, including the quality of the film. Bennett and Bennett[13] showed that the spectral emissivity of metallic films depends on the quality of the surface, the

Table 1 Hemispherical emittance data, with probable errors, at various sample temperatures (a_b = 0.98 ±0.01; $F \approx 1.0$)

	60°K	100°K	300°K
T_s, °K	60 ± 0.5	100 ± 0.7	300 ± 2.5
Q_c, w	(2.0 ± 0.15) × 10^{-5}	(1.60 ± 0.01) × 10^{-4}	(3.60 ± 0.018) × 10^{-2}
$\epsilon_s \times 10^4$	90 ± 10	105 ± 3	210 ± 7

Table 2 Calorimetric total hemispherical emittances, with probable errors, of vacuum-deposited gold films

Gold on Mylar			Gold on Kapton
470 Å	550 Å[a]	720 Å[b]	400 Å[c]
$\epsilon_s \times 10^4$, °K	$\epsilon_s \times 10^4$, °K	$\epsilon_s \times 10^4$, °K	$\epsilon_s \times 10^4$, °K
109 ± 8 61	114 ± 10 63	83 ± 7 63	188 ± 9 196
119 ± 3 88	129 ± 4 91	102 ± 3 90	204 ± 10 255
131 ± 4 129	152 ± 5 129	120 ± 2 132	212 ± 11 314
154 ± 5 162	156 ± 5 149	132 ± 4 166	
203 ± 6 253	212 ± 6 253	175 ± 5 259	
220 ± 7 307	244 ± 8 302	210 ± 6 312	

Gold on Copper			
400 Å[d]	520 Å[d]	4000 Å[d]	2500 Å[c]
$\epsilon_s \times 10^4$, °K	$\epsilon_s \times 10^4$, °K	$\epsilon_s \times 10^4$, °K	$\epsilon_s \times 10^4$, °K
97 ± 8 59	108 ± 9 59	85 ± 7 59	135 ± 7 201
121 ± 4 96	118 ± 4 96	96 ± 3 97	153 ± 8 255
158 ± 5 161	153 ± 5 163	118 ± 4 161	164 ± 8 302

[a] Thickness measured on film samples, adjacent to emittance specimen, 200 Å thickness variation observed across sheet, ±100 Å.
[b] Thickness measured on 1-in. square area from center of emittance specimen, ±50 Å.
[c] Thickness per supplier, measurement method not known.
[d] Thickness measured on monitors adjacent to emittance specimen, ±50 Å.

quality and type of the substrate material, the purity of the film, and the vacuum and the rate under which the film was deposited. The effects of the first three items could be neglected when discussing ϵ for the 2500 Å thick sample. The smoothness and the flatness of the film surface and the substrate will affect the spectral measurements much more than the total measurements. Also, the ratio of the length characterizing the roughness of the surface to the characteristic wavelength of the incident radiation will decrease rapidly as the temperature decreases. Thus, the effect of roughness is usually negligible at cryogenic temperatures. The effect of sample purity, for purities higher than 99.99%, was also found to be negligible.[13] The remaining item, i.e., the vacuum and the rate at which the film was deposited, however, is very important. For example, the spectral emissivity of metallic films deposited at a rate of 7 Å/sec and under high-vacuum conditions, 10^{-5} torr, could be two or three times higher than the emissivity of a similar film deposited under ultra-high-vacuum conditions, 10^{-9} torr. The rate at which the film is deposited is also an important factor. The higher the rate of deposition, the better and purer is the film. Measurements determining the effect of deposition rate on the film emissivity, however, are not available.

References

[1] Ruccia, F. E., Hinkley, R. B., and Reid, R. C., "Thermal Performance of Tank Applied Multilayer Insulation," *Advances in Cryogenic Engineering*, Vol. 12, Plenum Press, New York, 1967, pp. 218–24.

[2] Vliet, G. C. and Coston, R. M., "Thermal Energy Transport Parallel to the Laminations in Multilayer Insulation," *Advances in Cryogenic Engineering*, Vol. 13, Plenum Press, New York, 1968, pp. 671–679.

[3] Barnes, R. B. and Czerny, M., "Concerning the Reflection Power of Metals in Thin Layers for the Infrared," *Physical Review*, Vol. 38, 1931, pp. 338–345.

[4] Reuter, G. E. H. and Sondheimen, E. H., "The Theory of the Anomalous Skin Effect in Metals," *Proceedings of the Royal Society*, London, Ser. A, Vol. 195, 1948, pp. 336–364.

[5] Domoto, G. A., Boehm, R. F., and Tien, C. L., "Predictions of the Total Emissivity of Metals at Cryogenic Temperatures," *Advances in Cryogenic Engineering*, Vol. 14, Plenum Press, New York, 1968.

[6] Fuchs, K., "The Conductivity of Thin Metallic Films According to Electron Theory of Metals," Cambridge Philosophical Society, Vol. 34, 1938, pp. 100–108.

[7] Tien, C. L., Armaly, F. G., and Jagannathan, P. S., "Thermal Conductivity of Thin Metallic Films and Wires at Cryogenic Temperatures," *Proceedings of the Eighth Thermal Conductivity Conference*, Plenum Press, New York, 1969, pp. 13–20.

[8] Dingle, R. B., "The Anomalous Skin Effect and the Reflectivity of Metals, IV, Theoretical Optical Properties of Thin Metallic Films," *Physica*, Vol. 19, 1953, pp. 1187–1199.

[9] Armaly, F. G. and Tien, C. L., "Emissivities of Metals at Cryogenic Temperatures," *Proceedings of 4th International Heat Transfer Conference*, Vol. 3, RI.I, 1970.

[10] McCargo, M. and Greenberg, S. A., "Range of Low Energy Protons in Metals and Metal Oxides," submitted for publication.

[11] Ruccia, F. E. and Hinckley, R. B., "The Surface Emittance of Vacuum-Metallized Polyester Film," *Advances in Cryogenic Engineering*, Vol. 12, Plenum Press, New York, 1967, pp. 300–307.

[12] Caren, R. P., "Low-Temperature Emittance Determinations," *AIAA Progress in Astronautics and Aeronautics: Thermophysics and Temperature Control of Spacecraft and Entry Vehicles*, Vol. 18, edited by G. B. Heller, Academic Press, New York, 1966, pp. 61–73.

[13] Bennett, H. E. and Bennett, J. M., "Precision Measurements in Thin Film Optics," *Physics of Thin Films*, Vol. 4, Academic Press, New York, 1967, pp. 1–96.

Changes in the Vibration Characteristics due to Changes in the Structure

V. T. NAGARAJ*
Hindustan Aeronautics, Ltd., Bangalore, India

Nomenclature

a	=	see Eq. (10)
$F,\Delta F$	=	flexibility matrix and change in F, respectively
I	=	unit matrix
$M,\Delta M$	=	mass matrix and change in M, respectively
$Q(\lambda_r)$	=	"adjoint" matrix, see Eq. (9)
$U,\Delta U$	=	dynamic matrix and change in U, respectively
$x,\Delta x$	=	eigenvector and change in x, respectively
y	=	eigenrow
$\lambda,\Delta\lambda$	=	eigenvalue and change in λ, respectively
λ_A	=	$\lambda + \Delta\lambda$
ω	=	circular frequency (rad/sec)
$[\ ]$	=	row matrix
$\{\ \}$	=	column matrix
$[\ ]$	=	square matrix

Introduction

THE influence of small changes in a structure on its frequencies and mode shapes has been discussed by Krishna Murty and Viswa Murty.[1] They consider the following problem: the equations of motion of undamped vibrations of a system can be written as

$$([I] - \omega^2[F][M])\{x\} = 0 \qquad (1)$$

When $[F]$ and $[M]$ are changed to $[F + \Delta F]$ and $[M + \Delta M]$, they obtain expressions for $\Delta\omega^2$ and $\{\Delta x\}$ (the changes in the frequency and the mode shape) in terms of $[F]$, $[M]$, $[F + \Delta F]$, and $\{x\}$.

In the following sections, a simple procedure (method A) will first be given, which permits one to obtain quick estimates of the changes of the frequency and the mode shape. A more accurate method presented by Morgan[2] (method B) is de-

Received July 6, 1970; revision received September 10, 1970.
*Project Engineer, Vibrations and Aeroelasticity.